An adaptive tomographic technique to reconstruct local drop size distribution of liquid spray at multi-resolution

S. Tanchatchawan, P. Vallikul, P. Yongyingsakthavorn, Christophe Dumouchel

An adaptive tomographic technique to reconstruct local drop size distribution of liquid spray at multi-resolution

S. Tanchatchawan*, P. Vallikul, and P. Yongyingsakthavorn
Department of Mechanical and Aerospace Engineering
King Mongkut's University of Technology North Bangkok
Bangkok, Thailand

C. Dumouchel
UMR6614-CORIA-Université et INSA de Rouen
Rouen, France

Abstract

This paper proposes an adaptive deconvolution algorithm to reconstruct local drop-size distributions within liquid sprays at multiple resolutions by using the laser diffraction measurement data. The algorithm employs the strip integration by which the scattered light intensities from the local regions along the measured line-of-sight being integrated and scanned over the entire region at multiple resolutions. In the strip integration model, the contribution of the intensity scattered from each local region to the measured line-of-sight data is controlled by the area of intersection between the local region and the laser beam past the region. The algorithm allows the number of input line-of-sight measurement data to be larger than the number of local regions at some selective regions where the drop-size distributions being determined. This means that the local drop-size-distributions at the selected regions can be reconstructed at higher spatial resolutions than those at other regions. The algorithm has been tested by measuring drop-size-distributions of two water sprays whose drop-size distributions are spatially non-homogenous. The first spray is a two-dimensional like flat spray generated from an in-house designed nozzle "the single-hole triple disk nozzle" where the spray is constraint by the internal flow of the liquid before the injection. The second spray is a solid cone spray generated from a small industrial pressure swirl atomizer. It has been shown from the measurement results that the proposed algorithm is capable of reconstructing drop-size distribution of the liquid spray at multiple spatial resolutions.

*Corresponding author: songrit@tistr.or.th

Introduction

Line-of-sight data obtained from the measured forward scattered intensity of laser beams past through a spray has widely been used to reconstruct local intensity scattered from the points along the line-of-sight via the deconvolution processes [1-5]. In the deconvolution schemes, the measured line-of-sight intensity data, $\bar{I}$, was modeled as a line integration of the local forward scattered intensity, I, from local points along the laser beam; the integration begins at the laser source ($l = 0$)and ends at the detector ($l = L$), see Figure 1. In this sense, the local intensity, I, is the intensity per unit path length, L. Since the laser beam has a finite width,W, then the model local intensity has spatial resolution equal to one beam width, W.

Boyaval and Dumouchel (2001a) proposed to increase spatial resolutions of the reconstruction results by redefining the mathematical representation of the line-of-sight measurement data [6]. They modeled the single line-of-sight data as a combination of two line integrations of forward scattered light past regions a and b, see Fig. 1. In this model, two local intensities, $I_a$and I_b, of half width of the laser beam are spatially filled within one measurement. Then the local intensity in this two line integration model has higher spatial resolution than that of the one line integration model. With this concept in mind, multiple line integrations (more than two lines per one laser beam width) can also be included into the line-of-sight data. Local intensities for all line, however, have a single spatial resolution, equal to the number of local intensity by one beam width. If multiple resolutions of the local intensity were to be modeled then some weighting schemes on the width of the local region to which it represent are needed.

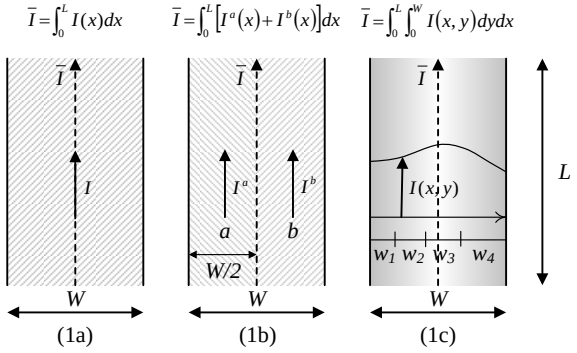

Figure 1. Line-of-sight models: single line integration (1a), double line integration(1b), and strip integration (1c)

In this paper we propose to model the line-of-sight data by the strip integration. The line-of-sight data is modeled by the integration of the local intensity along the line-of-sight, L, and over the beam-width, W,

$$\bar{I} = \int_0^L \int_0^W I(x,y)dydx \tag{1}$$

where $I(x,y)$ is the intensity per unit path-length per beam-width (or local intensity per unit area), see Fig. 1. The inner integrand can further be subdivided into n strips of arbitrary width,

$$W = w_1 + w_2 + \cdots w_n \tag{2}$$

Within each strip, the local intensity is $I(x,y_i)$ where $i = 1 \ldots n$. Therefore, the single line-of-sight data is modeled as the combination of n strip integrations,

$$I_L = \int_0^L \left(\int_0^{w_1} I(x,y_1)dy + \cdots + \int_{w_{i-1}}^{w_i} I(x,y_i)dy + \ldots + \int_{w_{n-1}}^{w_n} I(x,y_n)dy \right) dx. \tag{3}$$

The width, w_i, and the position, y_i, of the region of the local intensity can be modeled at arbitrary sizes. In other words, the local intensities can be modeled at multiple resolutions.

Measurement of drop-size distributions of a flat spray

The strip integration concept has been applied to measure drop-size distributions along a horizontal plane of a water spray, injected from a three-disc nozzle [7]. The nozzle operates at the pressure of 4 bar with corresponding mass flow rate of 7.4 kg/hr. The spray issued from the nozzle is a kind of flat-spray type. This is due to the asymmetrical flow inside the nozzle. The thickness of the spray is assumed constant along the span-wise direction while the drop-size distribution varies. Drop-size-distributions on a 10-cm-plane below the nozzle exit were determined in this study, see Figure 2.

Figure 2 shows that the span of the spray is 10 cm and that there are 16 laser beams scan across. The beam width is 10-mm. From the left edge, each laser beam is scanned 2.5 mm apart for 3 cm span such that the local intensities can be resolved at high resolution within this span. Beyond the 3-cm-span, each laser beam is scanned at 10 mm apart. the resolution of the local intensity within this region is coarser. The region of interest in this study is within the first span.

Based on (3), the relation between the path-integrated and the local scattered intensities can be written as

$$\bar{I}(y_i) = L \sum_{j=1}^{N} w_i(y_j) I(y_j) \tag{4}$$

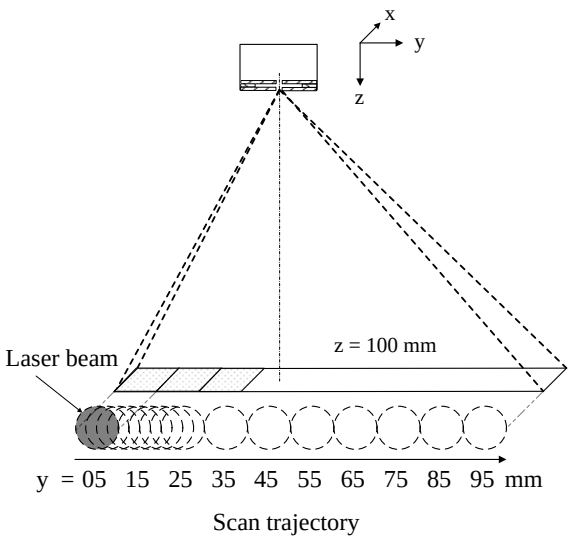

Figure 2. Description of flat water spray

The parameters appearing in (4) are illustrated in Figure 3. The path length, L, is constant while the strip's width, $w(y_j)$, depends on the overlapping distance between the widths of laser plane form area and the area of the local intensity at y_j. Note that for the flat spray the length L is finite such that the spray is homogenous along the line-of-sight measurements. The spray is non-homogenous across the width of the laser beam.

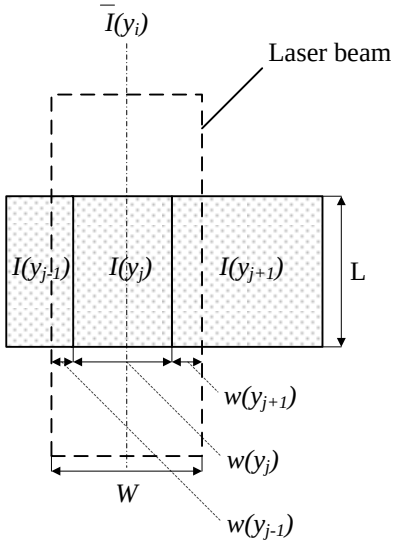

Figure 3. Conceptual drawing shows parameters involved in strip integration for the flat spray.

In (4), the path integrated data, $\bar{I}(y_i)$, where $i = 1 \ldots M$, are known line-of-sight measurement data. The local scattered intensities, $I(y_j)$, where $j = 1 \ldots N$, are unknowns. Since the number of measured line-of-sight data is greater than the number of unknowns, $M > N$, then the problem defined by (4) is an over determined problem. Maximum entropy technique [8] has been used to solve for the local intensities.

Once the local intensities had been solved, the local drop-size-distribution at the local region could be determined. Procedures to determine drop-size-distribution from the known local scattered intensities can be found in our earlier work [9]. The drop-size-distribution in this work is the volume frequency,

$$f_v(D_i) = \frac{1}{\Delta D_i} \frac{V_i}{\sum_{i=1}^{m} V_i} \tag{5}$$

The mean diameter, D_{32}, is the sauter mean diameter,

$$D_{32} = \frac{\sum_{i=1}^{m} N_i D_i^3}{\sum_{i=1}^{m} N_i D_i^2} \tag{6}$$

where i denotes the size class consider, N_i is the number of drops in size class i, D_i is the middle diameter of size class i, m is the number of class, ΔD_i is the width of class i and V_i is the liquid volume contained in class i

Figure 4 shows the measurement results of the mean diameters of the spray for three local regions near the left edge of the spray. The width of the local regions is equal to the width of the laser beam in other words the resolution of the local mean diameter is one to one (1:1).

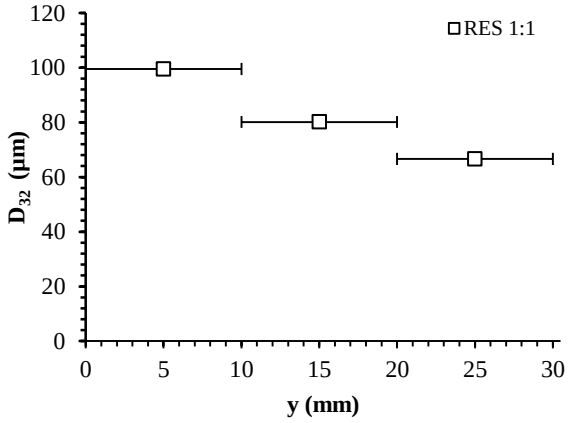

Figure 4. Means diameter of the three local regions from the left edge.

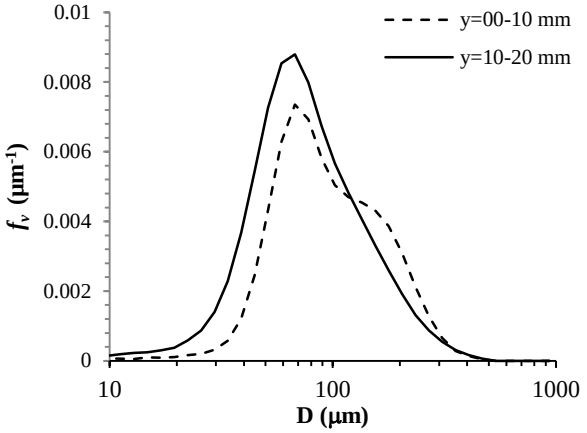

Figure 5. Drop-size-distribution of the first two local regions from the left edge.

Figure 5 shows the measurement results of drop-size-distribution of the first two local regions of the above case (shown in Figure 4), the local regions are between 0-10 mm and 10-20 mm. It can be seen that the drop-size-distribution has two modes at the edge region. Further away from the edge, the drop-size-distribution becomes single mode distribution.

Multi-resolutions reconstructions to determining mean diameters and drop-size-distributions have been performed within the regions between 0 to20 mm from the edge of the spray. The region was divided into four local regions. The first three are determined at resolution equal to 2.25 to 1 and the fourth region is determined at the resolution 1.5 to 1. Figure 6 shows the results of mean diameters as multi-resolutions reconstructions.

Figure 7 shows the resulting drop-size-distributions of the four regions. By measuring at higher resolutions one can resolve drop-size-distributions within a finer width. The drop-size-distributions obtained are consistent with those obtained at the coarser local regions.

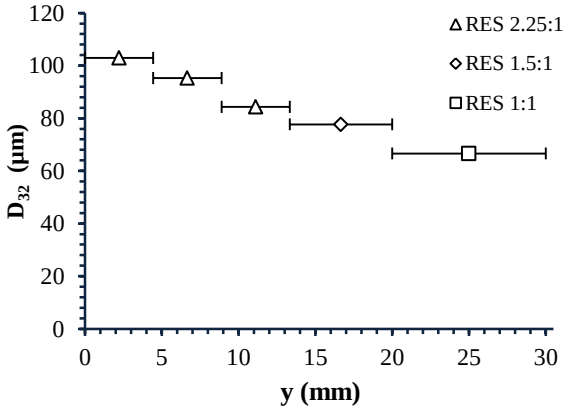

Figure 6. Mean diameters, measuring with multi-resolutions

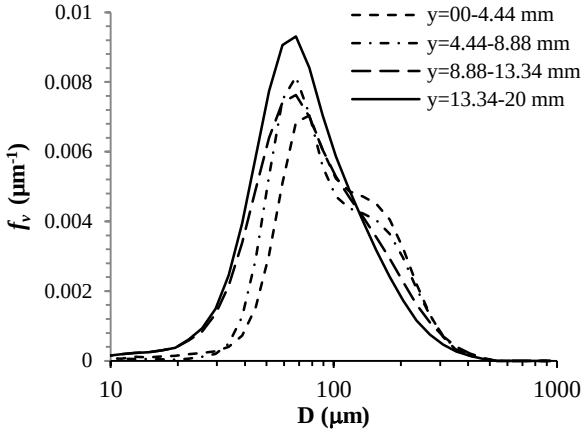

Figure 7. Drop-size-distributions, measuring with multi- resolutions

Measurement of drop-size-distributions of a solid cone spray

The pressure-swirl atomizer was used to generate an axi-symmetrical solid-cone water spray [9]. The measurement has been conducted on a cross-sectional plane of the spray at 7 cm below the nozzle exit. The injection pressure used is 12 bar giving the mass flow rate 4 kg/hr. Figure 8 shows schematic diagram of the spray and the measurement plane.

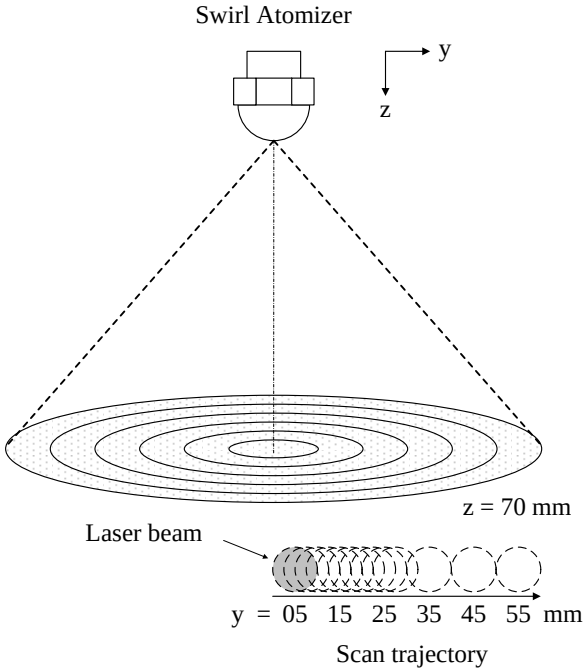

Figure 8. Schematic diagram of a solid-cone spray and the measurement plane

The axi-symmetrical plane has the radius of 60 mm and the line-of-sight measurements have been scanned across the half plane. Two scanned modes have been performed. Between 0 and 30 mm, each measured line-of-sight is 2.5 mm apart and beyond that each measurement is 10 mm apart.

In the axi-symmetrical spray, the local regions are modeled as $N-1$ concentric rings and a centre core where the local intensity within each region, $I(r_j)$, is assumed constant. Mathematical model of the line-of-sight, $\bar{I}(y_i)$, can be written based on (3) but in discrete form as

$$\bar{I}(y_i) = \sum_{j=1}^{N} A_{i,j}\, I(r_j) \qquad (7)$$

$A_{i,j}$ is the intersection area between the local concentric ring at $r_{j=1\ldots N}$ and the plan form area of the beam past $y_{i=1\ldots M}$. Figure 9 shows the pertinent parameters appearing in (7). Note that only half- length line-of-sights are shown in the Figure 9.

Figure 10 shows the reconstructed mean diameters for each local region whose width is equal to the width of the laser beam. The resolution of the reconstruction is one to one. It can be seen that the mean diameter increases from the center core toward the outer edge.
Figure 11 shows the corresponding drop-size-distributions within the local regions. It can be seen that there are important changes both in the mean diameters and in the widths when comparing the drop-size-distributions within concentric rings 5-15 mm and 15-25 mm. This means that there are steep variations between the two local regions. Reconstruction at higher resolutions within those local regions are needed.

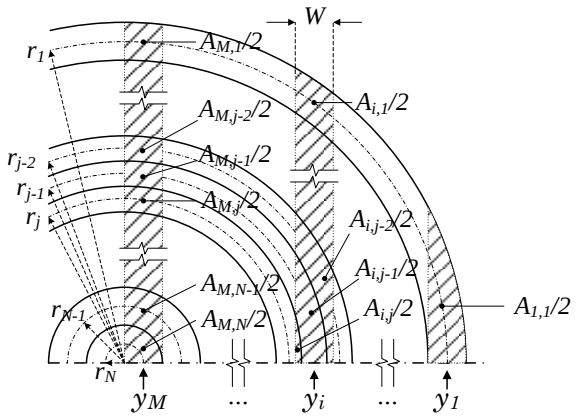

Figure 9. Drawing defines pertinent parameters relating line-of-sight and local intensity.

Reconstruction results of the mean diameters at multi resolutions are shown in Figure 12. It can be seen that the mean diameters increase with the radius; the values are consistent with the results in Figure 10. The reconstruction results show that within concentric rings 14-20 and 20-26 mm, the mean diameters are almost equal. Figure13 shows, however, that drop-size-distributions within the two regions have significantly different widths. Beyond the radius of 20 mm the width of the drop-size-distributions are broadened. Furthermore the incomplete local spray information in the previous case has been fulfilled.

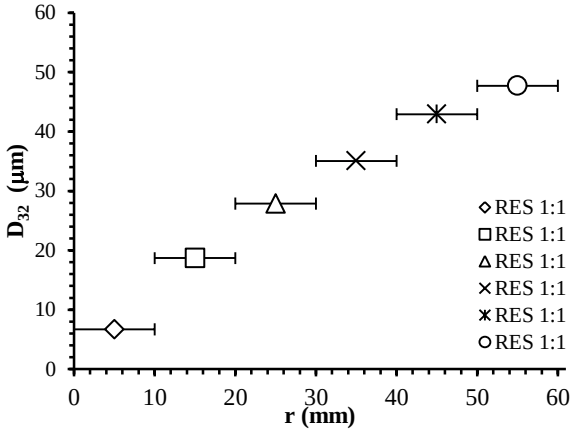

Figure 10. Mean diameters of solid cone spray, measuring with single resolution

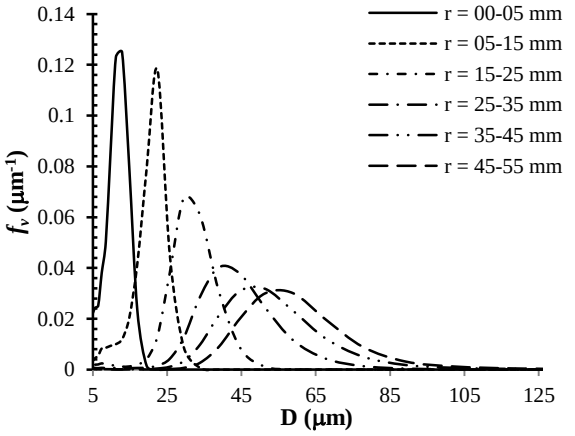

Figure 11. Drop-size-distributions of solid cone spray, measuring with single resolution

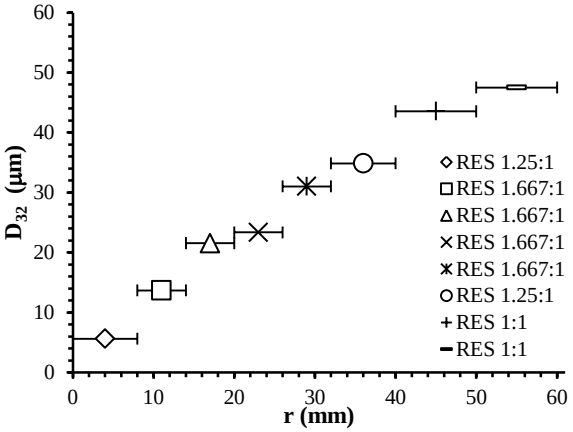

Figure 12. Mean diameters of solid cone spray, measuring with multi- resolutions

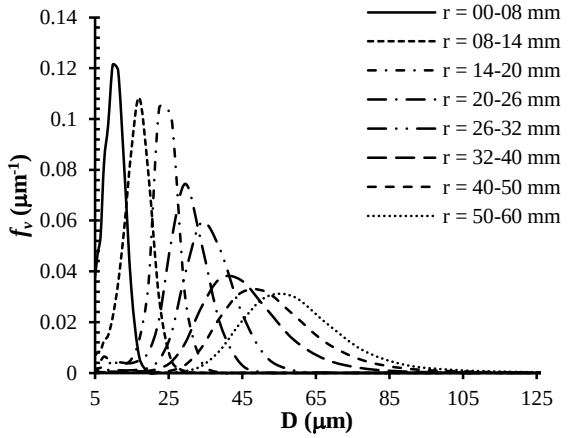

Figure 13. Drop-size-distributions of solid cone spray, measuring at multi- resolutions

Conclusions

The proposed adaptive tomographic reconstruction technique has been applied to reconstruct drop-size-distributions within different types of sprays. The developed algorithm is able to resolve the distributions at multiple resolutions. This is the main advantage of the proposed technique over the conventional techniques where the solutions obtained are at single (and often coarse) resolution and the adaptation of the width of the local reconstruction region is not possible. It has also been shown that by using the strip-area as the reconstruction basis, the algorithm can handle the different shapes of the local reconstructed regions, e.g. rectangular or circular ring areas.

Acknowledgements

The first author is being supported under the PhD scholarship program by the Ministry of Sciences and Technology (MOST), Thailand and Thailand Institute of Scientific and Technological Research (TISTR). Research facilities are partially provided by the Joint Graduate School of Energy and Environment, King Mongkut's University of Technology Thonburi and the Graduate School, King Mongkut's University of Technology North Bangkok.

References

1. Hammond, D.C., *Appl Opt* 20:493-499.
2. Yule, A.J., Seng, A.H., Felton, C., Ungut, P.G, and Chigier, A., *Eighteenth symposium (international) on combustion*, 1981, pp. 1501-1510.
3. Dodge, L.G., Rhodes, D.J., and Reitz, R.D., *Appl Opt* 26:2144-2154 (1987).
4. Drallmeier, J.A., Peters, J.E., *Atomization and Sprays* 4:135-138 (1994).
5. Lee, K., and Reitz, R.D., *Meas Sci Technol* 15: 509-519 (2004).
6. Boyaval, S., and Dumouchel, C., *ILASS-Europe*, Zurich, 2001a.
7. Dumouchel, C., Cousin, J., and Triballier, K., *Experiments in Fluids* 38:637-647 (2005).
8. Bevensee, R.M., *IEEE Trans Antennas Propag* AP-29:271-274 (1993).
9. Yongyingsakthavorn, Y., Vallikul, P., Fungtammasan, B., and Dumouchel C., *Exp Fluids* 42:471-481 (2007)